

Search for the Standard Model Higgs boson in the $H \rightarrow ZZ^* \rightarrow 4\ell$ decay channel with the ATLAS detector

Konstantinos Nikolopoulos*

On behalf of the ATLAS Collaboration

University of Birmingham,

Edgbaston, Birmingham, B15 2TT, United Kingdom

E-mail: konstantinos.nikolopoulos@cern.ch

The search for the Standard Model Higgs boson in the decay channel $H \rightarrow ZZ^{(*)} \rightarrow \ell^+\ell^-\ell'^+\ell'^-$, where $\ell, \ell' = e$ or μ , is presented using 4.8 fb^{-1} and 5.8 fb^{-1} of proton-proton collision data at centre-of-mass energies of 7 TeV and 8 TeV, respectively, recorded with the ATLAS detector at the Large Hadron Collider. The search is performed for Higgs boson masses between 110 and 600 GeV.

The Standard Model Higgs boson is excluded at 95% confidence level in the mass ranges 131–162 GeV and 170–460 GeV, while the expected exclusion ranges are 124–164 GeV and 176–500 GeV. An excess of events is observed around $m_H = 125 \text{ GeV}$, with a local significance of 3.4 standard deviations.

*36th International Conference on High Energy Physics,
July 4-11, 2012
Melbourne, Australia*

*Speaker.



1. Introduction

The search for the Standard Model (SM) Higgs boson [1–3] is a major aspect of the Large Hadron Collider (LHC) physics programme. Direct searches at the CERN Large Electron-Positron Collider excluded at 95% confidence level (CL) the production of a SM Higgs boson with mass, m_H , less than 114.4 GeV [4]. Searches at the Fermilab Tevatron $p\bar{p}$ collider excluded at 95% CL the region $147 \text{ GeV} < m_H < 179 \text{ GeV}$ [5]. At the LHC, the ATLAS experiment using up to 4.9 fb^{-1} of data at a centre-of-mass energy (\sqrt{s}) of 7 TeV excluded the m_H regions 112.9–115.5 GeV, 131–238 GeV and 251–466 GeV at 95% CL [6]. The CMS results based on up to 4.8 fb^{-1} of $\sqrt{s} = 7 \text{ TeV}$ data excluded at the 95% CL the m_H range 127–600 GeV [7].

The search for the SM Higgs boson through the decay $H \rightarrow ZZ^{(*)} \rightarrow \ell^+\ell^-\ell'^+\ell'^-$, where $\ell, \ell' = e$ or μ , provides good sensitivity over a wide mass range. The main background arises from continuum $ZZ^{(*)}$ production. For low masses, important background contributions arise from Z + jets and $t\bar{t}$ production, where the additional charged lepton candidates originate either from decays of hadrons with b - or c -quark content or from mis-identification of jets. The expected production cross sections for the SM Higgs boson, calculated up to next-to-next-leading order for the major production mechanisms, in pp collisions at $\sqrt{s} = 7$ and 8 TeV are compiled in Refs. [8, 9].

In the following, the updated ATLAS [10] search for the SM Higgs boson in the decay channel $H \rightarrow ZZ \rightarrow 4\ell$ is presented using 4.8 fb^{-1} of $\sqrt{s} = 7 \text{ TeV}$ and 5.8 fb^{-1} of $\sqrt{s} = 8 \text{ TeV}$ data [11], collected using single-lepton or di-lepton triggers and subjected to quality requirements.

2. Lepton Reconstruction/Identification and Event Selection

Electron reconstruction and identification in ATLAS is described in Ref. [12]. For the 2012 data taking, the electron reconstruction has been improved offering better performance at low transverse momentum (p_T). The track pattern recognition and fit [13] procedures were updated to account for energy losses due to bremsstrahlung, and the track-to-cluster matching algorithm was improved to be less sensitive to bremsstrahlung losses. The identification criteria were optimised for good performance in high pile-up conditions, and to profit from the new electron reconstruction.

Muon candidates are formed by matching reconstructed Inner Detector (ID) tracks with either complete or partial tracks reconstructed in the Muon Spectrometer (MS) [14]. If a complete track is present, the two independent momentum measurements are combined; otherwise the momentum is measured using the ID or the MS information alone. The muon reconstruction/identification coverage is extended by using tracks reconstructed in the forward region ($2.5 < |\eta| < 2.7$) of the MS, which is outside the ID coverage. For $|\eta| < 0.1$, which lacks MS geometrical coverage, ID tracks with $p_T > 15 \text{ GeV}$ are identified as muons using the profile of the associated energy deposits in the calorimeter.

This analysis searches for Higgs boson candidates by selecting two same-flavour, opposite-sign lepton pairs in an event. The leptons should arise from the same reconstructed primary vertex, defined as the reconstructed vertex with the highest $\sum p_T^2$ of associated tracks among the reconstructed vertices. Each electron (muon) must satisfy $p_T > 7 \text{ GeV}$ (6 GeV) and be measured in the pseudo-rapidity range $|\eta| < 2.47$ (2.7). The most energetic lepton in the quadruplet must satisfy $p_T > 20 \text{ GeV}$, and the second (third) lepton in p_T order must satisfy $p_T > 15 \text{ GeV}$ (10 GeV). The

leptons are required to be separated from each other by $\Delta R > 0.1$ (0.2) for same(different)-flavour. The invariant mass, m_{12} , of the di-lepton closest to the Z boson mass (m_Z), leading di-lepton, is required to be between 50 and 106 GeV. The invariant mass, m_{34} , of the sub-leading di-lepton is required to be in the range $m_{\min} < m_{34} < 115$ GeV, where m_{\min} depends on the reconstructed four-lepton invariant mass, $m_{4\ell}$, as shown in Table 1. All same-flavour opposite-charge di-lepton combinations in the quadruplet must satisfy $m_{\ell\ell} > 5$ GeV. Four different analysis sub-channels ($4e$, $2e2\mu$, $2\mu2e$, 4μ) ordered by the flavour of the leading di-lepton are defined.

Table 1: The lower thresholds applied to m_{34} for reference values of $m_{4\ell}$ [11]. For $m_{4\ell}$ values between these reference values the selection requirement is obtained via linear interpolation.

$m_{4\ell}$ [GeV]	≤ 120	130	150	160	165	180	≥ 190
m_{\min} threshold [GeV]	17.5	22.5	30	30	35	40	50

The Z +jets and $t\bar{t}$ background contributions are further reduced by applying impact parameter as well as track- and calorimeter-based isolation requirements on the leptons. The normalised track isolation is defined as the sum of the transverse momenta of good quality tracks, Σp_T , inside a cone of $\Delta R < 0.2$ around the lepton, excluding the lepton track, divided by the lepton p_T . Each lepton is required to have a normalised track isolation smaller than 0.15. The normalised calorimetric isolation for electrons is computed as the sum of the positive-energy topological clusters with a reconstructed barycenter falling in a cone of $\Delta R < 0.2$ around the candidate electron cluster, divided by the electron p_T . This is required to be less than 0.20, excluding the contributions from the candidate electron itself. For muons, the normalised calorimetric isolation discriminant is the sum of the calorimeter cells, ΣE_T , inside a cone of $\Delta R < 0.2$ around the muon direction, divided by the muon p_T . The cut value is 0.30 (0.15 when no ID track). For both the track- and calorimeter-based isolation contributions arising from other leptons in the quadruplet are subtracted. The transverse impact parameter divided by its uncertainty, the significance, is required to be lower than 3.5 (6.5) for all muons (electrons).

The combined signal reconstruction and selection efficiency for $m_H = 130$ GeV (360 GeV) is

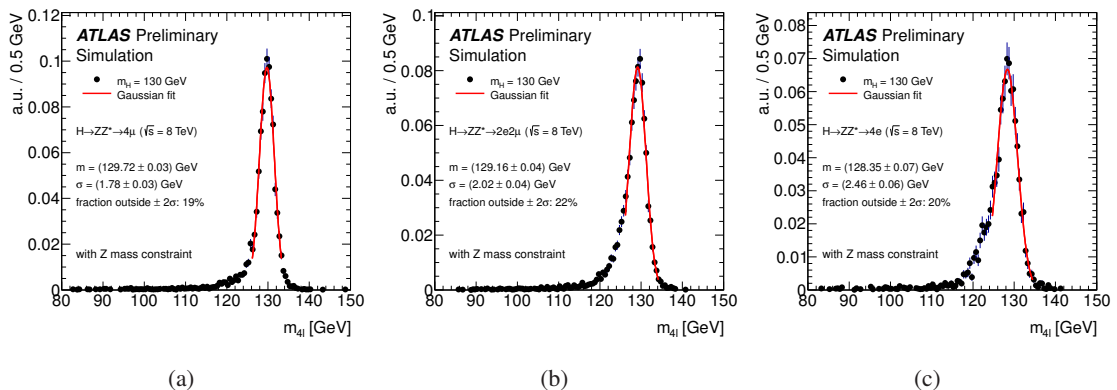


Figure 1: $m_{4\ell}$ distributions for simulated $H(130 \text{ GeV}) \rightarrow ZZ^* \rightarrow 4\ell$ events in the (a) 4μ , (b) $2e2\mu/2\mu2e$ and (c) $4e$ channel [11]. The fitted range is -2σ to 2σ (-1.5σ to 2.5σ) for the 4μ ($2e2\mu/4e$) channel. The slightly reduced mean values, due to radiative losses, are more explicit in channels with electrons [12].

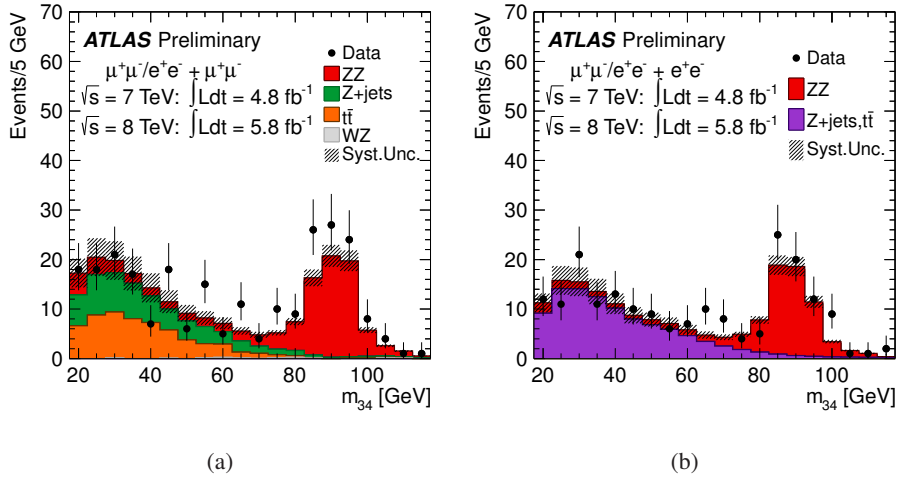


Figure 2: The m_{34} distributions for (a) $ll + \mu\mu$ and (b) $ll + ee$ events [11]. The kinematic selection of the analysis is applied. Isolation and impact parameter significance requirements are applied to the first lepton pair only. The MC is normalized to the data-driven background estimations.

41% (67%) for the 4μ channel, 27% (59%) for the $2e2\mu/2\mu2e$ channels and 23% (51%) for the $4e$ channel. The final discriminating variable for this search is $m_{4\ell}$. The invariant mass resolution is further improved by applying a Z -mass constraint, accounting for the Z boson line-shape and the experimental uncertainty in the di-lepton mass. Figure 1 presents the $m_{4\ell}$ distributions for a simulated signal sample with $m_H = 130$ GeV at $\sqrt{s} = 8$ TeV.

3. Background Estimation

The expected background yield for $ZZ^{(*)}$ production is estimated using MC simulation normalised to the theoretical cross section. For the $ll + \text{jets}$ and $t\bar{t}$ processes data-driven methods are applied. The background composition depends on the flavour of the sub-leading di-lepton and different approaches are taken for the $ll + \mu\mu$ and the $ll + ee$ final states. The data/MC comparison, after the data-driven methods have been employed is presented in Fig. 2.

3.1 $ll + \mu\mu$ background

The expected $t\bar{t}$ and $Z + \text{jets}$ (dominated by $Zb\bar{b}$) background events in the signal region are estimated using a control region obtained by removing the isolation requirements from the sub-leading muons, and require either of those muon to fail the impact parameter significance requirement. As shown in Fig. 3, the m_{12} distribution is fitted using a second order Chebychev polynomial for the $t\bar{t}$ component and a Breit-Wigner line-shape convolved with a Crystal-Ball resolution function for the $Z + \text{jets}$ component.

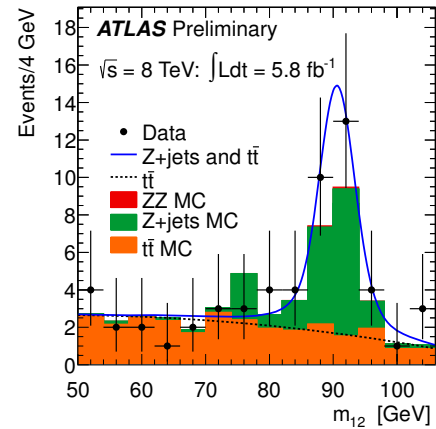


Figure 3: Distribution of m_{12} , for $\sqrt{s} = 8$ TeV, in the $ll + \mu\mu$ control region [11]. The fit to the $t\bar{t}$ and $Z + \text{jets}$ components is presented, along with the MC expectations.

These shapes are obtained from MC. The estimated yields in the control region are extrapolated to the signal region using an MC-based transfer factor. The MC description of the selection efficiency was verified using events with a Z boson and an extra muon.

The $t\bar{t}$ background is cross-checked using events with an $e^\pm\mu^\mp$ di-lepton with an invariant mass between 50 and 106 GeV, accompanied by an opposite-sign di-muon. A Z boson veto is applied. Isolation and impact parameter requirements are applied only to the leptons of the $e\mu$ pair. This method is found to give consistent expectations in the signal region.

3.2 $\ell\ell + ee$ background

A sample of reconstruction-level objects identified as electron candidates will contain true isolated electrons, electrons from heavy flavour semi-leptonic decays (Q), electrons from photon conversion (γ) or mis-identified light jets (f).

Table 2: The observed yields of the various reconstruction-based categories in the $\ell\ell + ee$ control region for $\sqrt{s} = 8$ TeV [11]. The MC expectations are also shown for comparison.

	$4e$		$2\mu 2e$	
	Data	MC	Data	MC
EE	32	22.7 ± 4.8	31	24.9 ± 5.0
EC	6	6.0 ± 2.5	2	1.9 ± 1.4
EF	18	19.0 ± 4.4	26	15.3 ± 3.9
CE	4	8.8 ± 3.0	6	5.1 ± 2.3
CC	1	5.3 ± 2.3	6	4.2 ± 2.0
CF	12	8.8 ± 3.0	15	15.3 ± 3.9
FE	16	5.7 ± 2.4	12	8.4 ± 2.9
FC	6	6.5 ± 2.6	7	4.3 ± 2.1
FF	12	17.4 ± 4.2	16	33.6 ± 5.8
Total	107	100 ± 10	121	113 ± 11

An $\ell\ell + ee$ background control region is formed by relaxing the electron selection criteria for the sub-leading di-electron. The electron-candidates are separated into the following reconstruction-based categories: electron-like (E), conversion-like (C) and fake-like (F), using appropriate discriminating variables [15], like the fraction of high threshold hits in the Transition Radiation Tracker (R_{TTR}) and the number of b -layer hits ($n_{\text{hits}}^{\text{b-layer}}$). The numbers of observed events in each category (the electron-candidates are p_{T} -ordered) of the control region are presented in Table 2. The extrapolation of the background yield of each category to the signal region is obtained from MC. As a cross-check the method is applied to a sim-

ilar control region containing same-sign sub-leading di-electrons.

The $\ell\ell + ee$ background is also estimated using a control region with same-sign sub-leading di-electrons, where the three highest p_{T} leptons satisfy all the analysis criteria and the remaining electron is required to fulfill looser criteria. A simultaneous fit of templates, obtained from the $n_{\text{hits}}^{\text{b-layer}}$ and the R_{TTR} distributions, is used to estimate the yields for the different truth components: f, γ and Q. The templates used are obtained from MC. Finally, the $\ell\ell + ee$ background is also estimated by performing the full analysis but selecting same-sign pairs for the sub-leading di-electrons. All of these methods were found to give consistent results.

4. Systematic uncertainties

The muon identification and reconstruction efficiency uncertainty results in a relative acceptance uncertainty of the signal and the $ZZ^{(*)}$ background which is uniform over the mass range of interest, and amounts to $\pm 0.16\%$ ($\pm 0.12\%$) for the 4μ ($2e2\mu$) channel. The uncertainty of the

electron identification efficiency results in a relative acceptance uncertainty of $\pm 3.0\%$ ($\pm 1.7\%$) for the $4e$ ($2e2\mu$) channel at $m_{4\ell} = 600$ GeV and reaches $\pm 8.0\%$ ($\pm 4.6\%$) at $m_{4\ell} = 110$ GeV. The effects of muon momentum resolution and scale uncertainty are found to be negligible. The effect of the uncertainty of the energy resolution for electrons is negligible, while the uncertainty of the electron energy scale results in an uncertainty of less than $\pm 0.7\%$ ($\pm 0.4\%$) on the mass scale of the $m_{4\ell}$ distribution for the $4e$ ($2e2\mu$) channel. The selection efficiency of the isolation and impact parameter requirements is studied using data for both isolated and non-isolated leptons, and the simulation is found to be in good agreement. The theory-related systematic uncertainties, for the signal and $ZZ^{(*)}$ background, are discussed in Refs. [8, 9]. The uncertainty on the integrated luminosity is $\pm 1.8\%$ ($\pm 3.6\%$) [16, 17] for the 2011 (2012) dataset.

5. Results

The expected $m_{4\ell}$ distributions for the total background and several signal hypotheses are compared to the data in Fig. 4. In Table 3 the observed and expected events are presented, in a window of ± 5 GeV around various hypothesized Higgs boson masses.

Upper limits are set on the Higgs boson production cross section at 95% CL, using the CL_s modified frequentist formalism [18] with the profile likelihood ratio test statistic [19]. The test statistic is evaluated using an unbinned maximum-likelihood fit of signal and background models to the observed $m_{4\ell}$ distribution. Figure 5(a) shows the observed and expected 95% CL cross

Table 3: Expected signal and background, and the observed events, within ± 5 GeV of a given m_H [11].

m_H	4μ			$2e2\mu$			$4e$		
	exp. signal	exp. bkg	obs	exp. signal	exp. bkg	obs	exp. signal	exp. bkg	obs
120	1.16 ± 0.15	1.07 ± 0.07	4	1.29 ± 0.19	1.93 ± 0.18	3	0.50 ± 0.07	1.39 ± 0.19	2
125	2.09 ± 0.28	1.30 ± 0.08	6	2.28 ± 0.31	2.19 ± 0.21	5	0.89 ± 0.13	1.59 ± 0.22	2
130	3.26 ± 0.43	1.44 ± 0.08	3	3.51 ± 0.49	2.28 ± 0.21	3	1.33 ± 0.21	1.70 ± 0.22	1

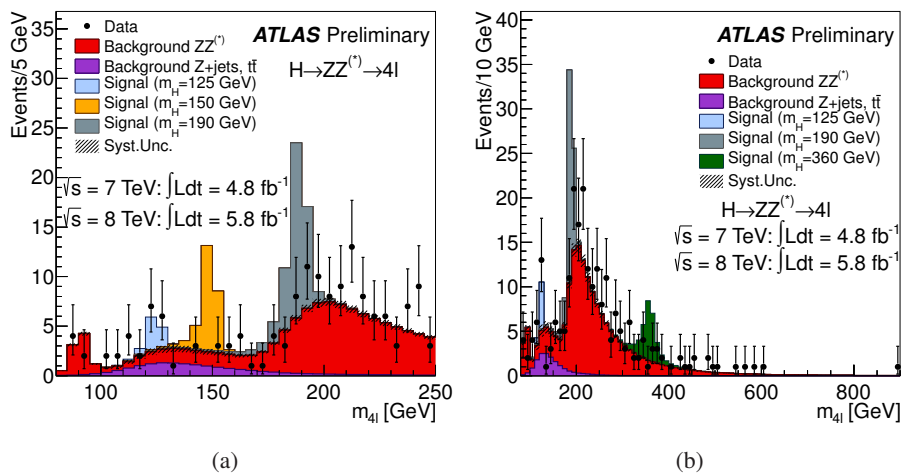


Figure 4: The $m_{4\ell}$ distribution for the selected candidates compared to the background expectation in the (a) 80–250 GeV and (b) full mass range [11]. The expected signal for several m_H hypotheses is also shown.

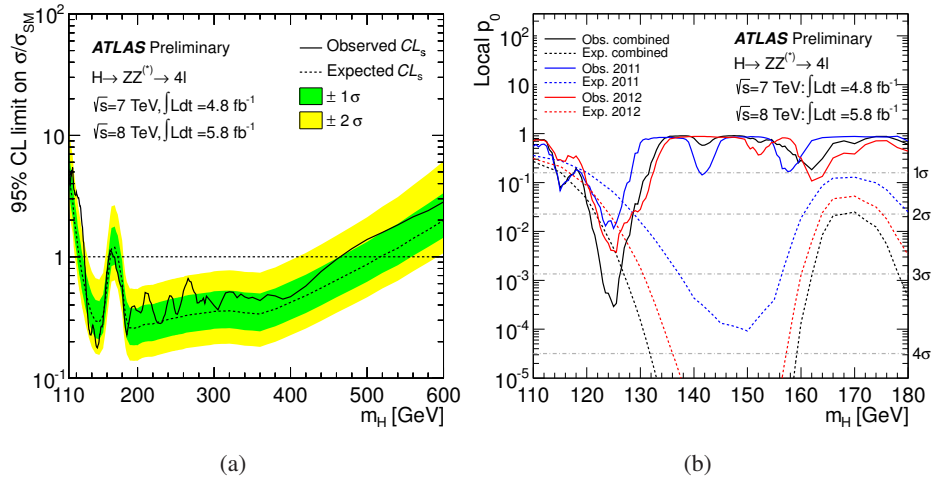


Figure 5: The expected (dashed) and observed (full line) 95% CL upper limits on the SM Higgs boson production cross section as a function of m_H , divided by the expected SM Higgs boson cross section [11]. The green and yellow bands indicate the expected limits with $\pm 1\sigma$ and $\pm 2\sigma$ fluctuations, respectively.

section upper limits, as a function of m_H . The mass ranges 131–162 GeV and 170–460 GeV are excluded at 95% CL, while the expected exclusion ranges are 124–164 GeV and 176–500 GeV.

In Fig. 5(b) the local p_0 , obtained using the asymptotic approximation [19], is presented as a function of the m_H hypothesis. The lowest local p_0 value is 0.029% 3.4 standard deviations (σ), at $m_H = 125$ GeV. No significant modification of the observed and expected p_0 in the low m_H region was observed, when the SM $ZZ^{(*)}$ normalisation was obtained directly from data. Correcting the above p_0 value for the *look-elsewhere effect* [20], using the mass range between 110 GeV and 141 GeV, results to a *global* p_0 of 0.65%, or 2.5 σ . For high mass ($m_H > 160$ GeV), the lowest p_0 is 1.9% (2.1 σ), at $m_H = 266$ GeV.

The signal strength parameter $\mu = \sigma/\sigma_{SM}$ is estimated to be 1.3 ± 0.6 at $m_H = 125$ GeV. Figure 6 presents the best μ and m_H fit and the profile likelihood ratio contours that asymptotically correspond to 68% and 95% CL.

6. Summary

A search for the SM Higgs boson in the decay channel $H \rightarrow ZZ^{(*)} \rightarrow 4\ell$ based on 4.8 fb^{-1} of data recorded with the ATLAS detector at $\sqrt{s} = 7$ TeV during 2011 and 5.8 fb^{-1} recorded at $\sqrt{s} = 8$ TeV during 2012 has been presented. The SM Higgs boson is excluded at 95% CL in the mass ranges 131–162 GeV and 170–460 GeV. An excess of events is observed around $m_H = 125$ GeV, whose p_0 value is 0.029% or 3.4 standard deviations.

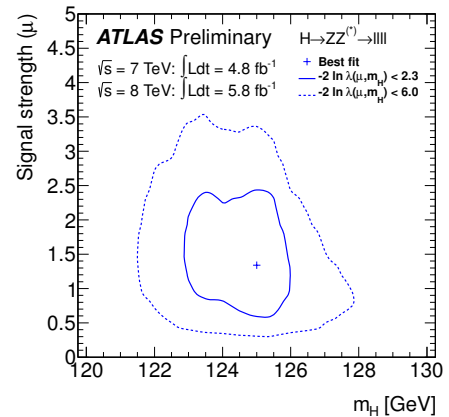


Figure 6: The (μ, m_H) plane with the best fit value and likelihood ratio contours that, asymptotically, correspond to 1 and 2 σ [11].

References

- [1] F. Englert and R. Brout, *Broken Symmetry and the Mass of Gauge Vector Mesons*, Phys. Rev. Lett. **13** (1964) 321–323.
- [2] P. W. Higgs, *Broken symmetries, massless particles and gauge fields*, Phys. Lett. **12** (1964) 132–133.
- [3] G. S. Guralnik, C. R. Hagen, and T. W. B. Kibble, *Global Conservation Laws and Massless Particles*, Phys. Rev. Lett. **13** (1964) 585–587.
- [4] LEP Working Group for Higgs boson searches, ALEPH, DELPHI, L3 and OPAL Collaborations, *Search for the standard model Higgs boson at LEP*, Phys. Lett. **B 565** (2003) 61–75.
- [5] T. T. N. Physics and H. W. Group, *Combined CDF and D0 Search for Standard Model Higgs Boson Production with up to 10.0 fb^{-1} of Data*, (2012). arXiv:1203.3774 [hep-ex].
- [6] ATLAS Collaboration, *Combined search for the Standard Model Higgs boson using up to 4.9 fb^{-1} of pp collision data at $\sqrt{s} = 7 \text{ TeV}$ with the ATLAS detector at the LHC*, Phys. Lett. **B710** (2012) 49–66.
- [7] CMS Collaboration, *Combined results of searches for the standard model Higgs boson in pp collisions at $\sqrt{s} = 7 \text{ TeV}$* , Phys. Lett. **B710** (2012) 26–48.
- [8] LHC Higgs Cross Section Working Group, S. Dittmaier, C. Mariotti, G. Passarino, and R. Tanaka (Eds.), *Handbook of LHC Higgs cross sections: 1. Inclusive observables*, 2011. arXiv:1101.0593 [hep-ph].
- [9] LHC Higgs Cross Section Working Group, S. Dittmaier, C. Mariotti, G. Passarino, and R. Tanaka (Eds.), *Handbook of LHC Higgs Cross Sections: 2. Differential distributions*, 2012. arXiv:1201.3084 [hep-ph].
- [10] ATLAS Collaboration, *The ATLAS Experiment at the CERN Large Hadron Collider*, JINST **3** (2008) S08003.
- [11] ATLAS Collaboration, *Observation of an excess of events in the search for the Standard Model Higgs boson in the $H \rightarrow ZZ^{(*)} \rightarrow 4\ell$ channel with the ATLAS detector*, ATLAS-CONF-2012-092 (2012).
- [12] ATLAS Collaboration, *Electron performance measurements with the ATLAS detector using the 2010 LHC proton-proton collision data*, Eur. Phys. J. **C72** (2012) 1909.
- [13] ATLAS Collaboration, *Improved electron reconstruction in ATLAS using the Gaussian Sum Filter-based model for bremsstrahlung*, ATLAS-CONF-2012-047 (2012).
- [14] ATLAS Collaboration, *Measurement of the $W \rightarrow \ell\nu$ and $Z/\gamma^* \rightarrow \ell\ell$ production cross sections in proton-proton collisions at $\sqrt{s} = 7 \text{ TeV}$ with the ATLAS detector*, JHEP **12** (2010) 060.
- [15] ATLAS Collaboration, *Measurements of the electron and muon inclusive cross-sections in proton-proton collisions at $\sqrt{s} = 7 \text{ TeV}$ with the ATLAS detector*, Phys. Lett. **B707** (2012) 438–458.
- [16] ATLAS Collaboration, *Luminosity Determination in pp Collisions at $\sqrt{s} = 7 \text{ TeV}$ Using the ATLAS Detector at the LHC*, Eur. Phys. J. **C 71** (2011) 1630.
- [17] ATLAS Collaboration, *Luminosity Determination in pp Collisions at $\sqrt{s} = 7 \text{ TeV}$ using the ATLAS Detector in 2011*, ATLAS-CONF-2011-116 (2012).
- [18] A. L. Read, *Presentation of search results: The CL_s technique*, J. Phys. **G 28** (2002) 2693–2704.
- [19] G. Cowan, K. Cranmer, E. Gross, and O. Vitells, *Asymptotic formulae for likelihood-based tests of new physics*, Eur. Phys. J. **C 71** (2011) 1554, arXiv:1007.1727 [physics.data-an].
- [20] E. Gross and O. Vitells, *Trial factors for the look elsewhere effect in high energy physics*, Eur. Phys. J. **C 70** (2010) 525–530.